Detailed Process of Adsorption of Alkanes and Alkenes on Zeolites

Eisuke Yoda,[†] Junko N. Kondo, and Kazunari Domen*[,‡]

Chemical Resources Laboratory, Tokyo Institute of Technology, 4259 Nagatsuta, Midori-ku, Yokohama 226-8503, Japan

Received: June 17, 2004; In Final Form: September 9, 2004

The adsorption of alkanes and alkenes on zeolites is investigated by comparing the adsorption characteristics for three types of zeolite: ferrierite, ZSM-5, and mordenite. The activation energy for the diffusion of propane and *n*-butane on ferrierite and the heat of adsorption of C_2-C_4 alkanes and alkenes on zeolites and silica are estimated based on Fourier transform infrared spectroscopy, and the diffusion processes in the micropores are elucidated by comparing the results with previously reported activation energies for *n*-butene diffusion. The adsorption of 1-butene on mordenite is also examined. The structure and process of experimentally observable adsorption is found to differ depending on the type of zeolite and adsorbing molecule, reflecting differences in the sizes of molecules and pores. This differing behavior is utilized to interpret the elementary adsorption processes of alkanes and alkenes on zeolites.

1. Introduction

The micropores of zeolites are of a similar size to a range of hydrocarbon molecules, and a number of shape-selective reactions have been utilized in practical applications.[1] However, the relationship between pore size and the restriction of reactions through steric hindrances has yet to be adequately understood. Our group has studied the adsorption of alkenes on zeolites at below room temperature, and a number of adsorption structures were identified for one type of alkene.[2,3] The pore size of zeolites was also found experimentally to affect the adsorption sites and the structure of the alkene adsorption complex,[4−7] and the reactions of alkenes in zeolites exhibited a dependence on pore size.[4,8,9]

When molecules react in the micropores of zeolites, the molecules must exchange sites. Therefore, detailed knowledge of the motion of molecules inside the micropores of zeolites is necessary in order to understand the reaction mechanisms that occur on zeolites. A range of experimental techniques have been used to measure the diffusivity in zeolites, including the frequency response,[10] pulsed field gradient (PFG) nuclear magnetic resonance (NMR),[11] zero-length column (ZLC),[12] quasi-elastic neutron scattering (QENS),[13−15] positron emission profiling (PEP),[16] one-dimensional-exchange ^{13}C NMR methods,[17] and Fourier transform infrared spectroscopy (FTIR).[18,19] Molecular simulations have also become a powerful tool for studying adsorption on zeolites, and a number of different methods have been reported.[20−24] The shape selectivity (pore size) and density and type of Brønsted acid sites (BASs) are considered to affect the diffusion process. However, previous studies only reported the diffusivity of molecules, and the relation between those characteristics of zeolites and diffusion process was not discussed. In other words, the elementary step of diffusion in zeolitets was not clarified. Thus, the elementary diffusion process in zeolites has yet to be clarified. In our previous study, the intrusion and diffusion of *n*-butene into the micropores of ferrierite were examined by Fourier transform infrared (FTIR) spectroscopy, yet the details of the elementary diffusion process could not be elucidated.[25,26]

Alkene molecules entering the micropores of zeolites are reported to adsorb onto the OH groups (Si−OH−Al) of BASs by forming a hydrogen bond via the π-electron of the C═C bond (π-adsorption) as the most stable adsorption structure.[27] However, in the case of alkene adsorption in the micropores of ZSM-5 zeolite below 200 K, interaction between the alkyl groups of alkene and BASs (alkyl adsorption) and between alkene molecules and pore walls (wall adsorption) were observed (Figure 1).[3,4] In the IR spectra of 1-butene adsorbed on D−ZSM-5 at 166−201 K (Figure 2), a dip appears at 2671 cm^{-1} due to a decrease in isolated acidic OD groups, and a peak at 2589 cm^{-1} emerges due to acidic OD groups hydrogen bonded to the alkyl groups of 1-butene, representing alkyl adsorption. The ν(C═C) band of 1-butene at 1642 cm^{-1} is also apparent in these spectra. Increasing the temperature only slightly eliminates the interaction with acidic OD groups, although adsorbed 1-butene remained on the ZSM-5, suggesting the adsorption of 1-butene onto the pore walls of the zeolite. The ν(C═C) band at 1642 cm^{-1} also persists at slightly elevated temperature. At 201 K, the dip at 2671 cm^{-1} is also present, while a peak at 2302 cm^{-1} emerges due to acidic OD groups interacting with the π-electron of 1-butene. The ν(C═C) band at 1642 cm^{-1} shifted to 1627 cm^{-1} through interaction of the π-electrons with acidic OD groups. These spectral features suggest the energy diagram shown in Figure 1.

For ferrierite, which has much smaller pores than ZSM-5, *n*-butene has been observed to adsorb onto silanol groups on the external surface via the π-electrons of the C═C bond.[25] Although wall adsorption and alkyl adsorption were not observed experimentally, these two processes are expected to occur in the micropores of ferrierite during the migration of molecules. A general energy diagram for alkene adsorbed on zeolites is shown in Figure 3. In the case of alkane adsorption,

* To whom correspondence should be addressed. E-mail: kdomen@res.titech.ac.jp.

[†] Present address: Graduate School of Medicine and Engineering, Yamanashi University, Takeda, Kofu 400-8511, Japan.

[‡] Present address: Department of Chemical System Engineering, School of Engineering, The University of Tokyo, 7-3-1 Hongo, Bunkyo-ku, Tokyo 113-8656, Japan.

10.1021/jp047376+ CCC: $30.25
Published on Web 01/07/2005

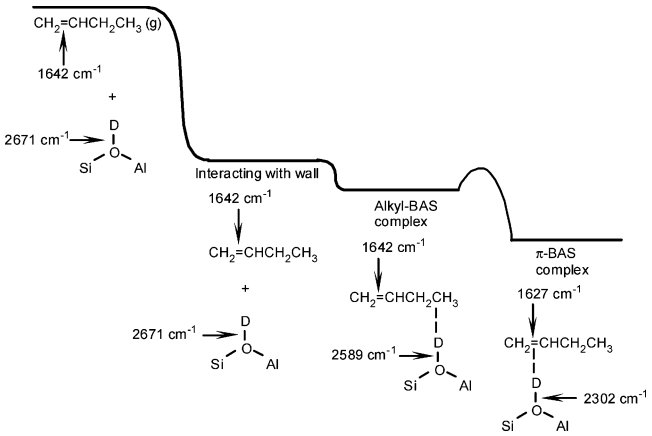

Figure 1. Energy diagram for 1-butene adsorbed on D−ZSM-5.

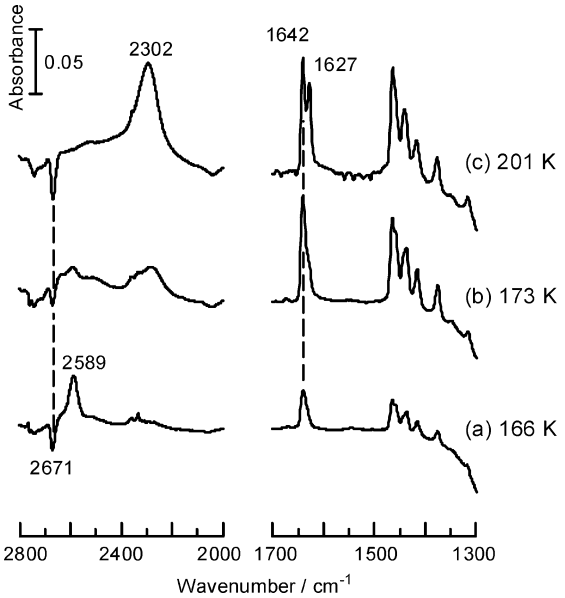

Figure 2. IR spectra of 1-butene adsorbed on D−ZSM-5 at 155 K followed by evacuation and heating: (a) 166, (b) 173, and (c) 201 K.

the most stable adsorption state is alkyl adsorption,[25,28−30] as alkanes do not possess π-electrons.

Although diffusion processes have been observed for ferrierite, the observations gave rise to a large number of possible interpretations for the energy barriers. The heat of adsorption on BASs may correspond to the activation energy for diffusion, since the molecules with the most stable interaction with BASs should be released from the BASs during the initial stage of diffusion. As the adsorption of molecules is also considered to be affected by the pore structure, diffusion in the micropores of zeolites is expected to be affected by the relative size of the pores and molecules in addition to the strength of Brønsted acidity. In such a case, the activation energy for diffusion should correspond to Figure 3a, which implies that the activation energy for diffusion will be almost the same for both alkanes and alkenes of the same size. On the other hand, if the desorption of alkene from BASs is the rate-determining step of diffusion (Figure 3b), the activation energy for diffusion should be dependent on the heat of adsorption for alkene. In this case, because the micropores are assumed to be sufficiently large compared to the size of *n*-butene isomers, the differences in the activation energies for migration among *n*-butene isomers on the walls of micropores are expected to be small compared with that of butane. However, as the heat of alkene adsorption onto BASs has yet to be reported due to the reaction of alkenes on BASs, it has not been clarified whether the difference in the heat of adsorption is related to the activation energies for diffusion based on the results of *n*-butene adsorption. In this study, the adsorption processes for alkanes on ferrierite are examined, and the details of the adsorption, diffusion, and migration of hydrocarbon molecules inside zeolite pores is clarified by comparing the results with the known adsorption processes for alkene. The differences in elementary adsorption with pore size are also discussed by comparing the results for three zeolites: mordenite, ZSM-5, and ferrierite.

2. Experimental Section

2.1. Samples and Pretreatment. Ferrierite (Tosoh; Si/Al = 8.5), mordenite (HM20, Catalysis Society of Japan; Si/Al = 9.95), H−ZSM-5 (Sumitomo Chemical; Si/Al = 50), and amorphous silica (Aerosil Nippon) were used as catalysts. About 30 mg of each catalyst was pressed into a self-supporting disk (20 mm in diameter) and placed in a quartz IR cell connected to a conventional closed gas-circulation system. The sample disk was pretreated at 773 K under 100 Torr of oxygen for 1 h, and then evacuated for 10 min to remove surface impurities. The sample was further pretreated at 673 K under 100 Torr of hydrogen for 1 h, and then cooled under evacuation. In some experiments, the disk was pretreated at 673 K under 100 Torr of deuterium to deuterate the acidic OH of zeolites to OD groups and thereby avoiding overlap between the OH band of the BASs interacting with the alkene and the ν(CH) bands of adsorbed alkene species.

2.2. IR Measurement. IR spectra were measured using a Jasco FT-IR 7300 spectrometer with a mercury cadmium telluride (MCT) detector. All spectra were collected at a resolution of 4 cm^{-1} and an average of 64 scans.

2.2.1.Gradual Warming under Evacuation. The IR spectra of the pretreated zeolites were measured at certain temperatures as the samples were cooled under evacuation from room temperature to 170 K as background spectra. This procedure accounts for the change of the background spectra with temperature, and in particular the shift of band due to acidic OH groups to higher frequencies with decreasing temperature.[31] About 20 μmol of alkane (ethane, propane, and *n*-butane) and alkene (1-butene) were introduced to the zeolites followed by evacuation at 170 K. IR spectra were then measured while the specimens were gradually warmed under evacuation. The evacuation condition ensured that only the species that were irreversibly adsorbed onto zeolites were observed by IR spectroscopy. Background-subtracted spectra are shown in the figures, in which peaks represent an increase in the number density of species after adsorption, and dips represent a decrease in the density of the corresponding species.

2.2.2. Adsorption Histories. Un-deuterated ferrierite was used as a catalyst for the quantitative analysis of adsorption. Known amounts of propane and *n*-butane were introduced to the pretreated ferrierite between 233 and 263 K, and the IR spectra of alkane adsorbed within the micropores of the ferrierite were obtained over time in the presence of alkane molecules in the gas phase (1.2 Torr) at a constant temperature.

2.2.3. Heat of Adsorption. Ferrierite, ZSM-5, and amorphous silica were used as catalysts for the measurement of the heat of alkane adsorption. The heat of C_2-C_4 alkane adsorption on acidic OH groups was measured for ferrierite and ZSM-5, and the heat of C_2-C_4 alkene and alkane adsorption was measured for SiO_2. The pretreated ferrierite, ZSM-5, and SiO_2 disks were exposed to gaseous hydrocarbon molecules at a constant temperature, and adsorption isotherms were measured at several

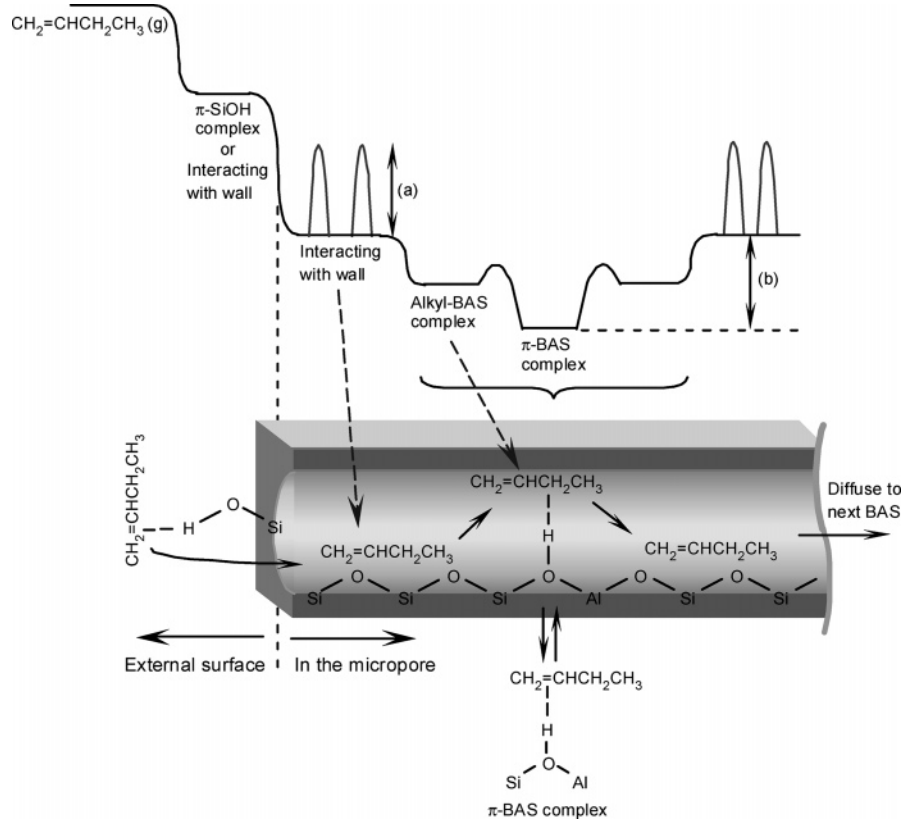

Figure 3. Energy diagram for 1-butene adsorbed on acidic OH groups in micropores of ferrierite from the gas phase. The activation energy of diffusion in micropores depends on (a) the size of molecules and pores, and (b) desorption of 1-butene from BASs.

TABLE 1: Experimental Conditions for the Estimation of Heats of Adsorption

catalysts	adsorbents	temp/K	press./Torr
SiO_2	ethane	223−253	0−100
	propane	223−253	0−60
	n-butane	233−263	0−15
	isobutane	233−263	0−30
	ethene	233−263	0−50
	propene	233−263	0−50
	1-butene	233−263	0−15
	cis-2-butene	243−273	0−15
	trans-2-butene	243−273	0−15
ferrierite	ethane	253−313	0−20
	propane	333−393	0−20
	n-butane	333−393	0−20
ZSM-5	ethane	253−313	0−15
	propane	293−353	0−15
	n-butane	313−373	0−10
	isobutane	313−373	0−15

temperatures. Fractional coverage was estimated by integrating the ν(OH) bands of BASs of the zeolites and silanol groups of the SiO_2. The experimental conditions are summarized in Table 1.

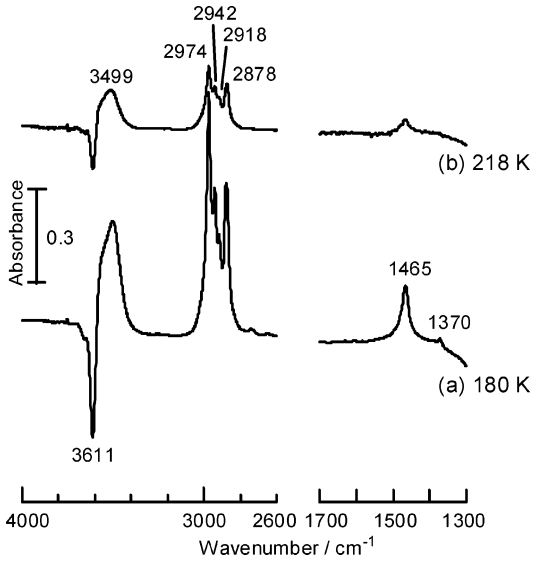

Figure 4. IR spectra of ethane on ferrierite introduced at 170 K followed by gradual warming under evacuation: (a) 180 and (b) 218 K.

3. Results and Discussion

3.1. Adsorption of Alkanes and Alkenes within the Micropores of Ferrierite. *3.1.1. Alkane Adsorption on Internal and External Surfaces of Ferrierite.* The amount of alkane adsorbed in the micropores of the samples was estimated from the amount of interacting acidic OH groups. The acidic OH groups of ferrierite have been confirmed to be confined to the micropores, while the silanol groups have been shown by pyridine adsorption to be present only on the external surface.[7] As pyridine cannot enter the micropores of ferrierite below room temperature, pyridine adsorption experiments allow for such a distinction, and it has been shown that the pyridine interacts with all silanol groups but not with acidic OH groups under these conditions. Therefore, molecules adsorbed on acidic OH groups can be confidently placed within the micropores, while molecules adsorbing onto silanol groups will be located on the external surface.

The general behavior of adsorption and reaction processes on catalysts can be determined from the spectral changes that occur during gradual warming. The IR spectra of ethane adsorbed on ferrierite are shown in Figure 4. The dip at 3611 cm^{-1} is attributable to ν(OH) of BASs and results from the

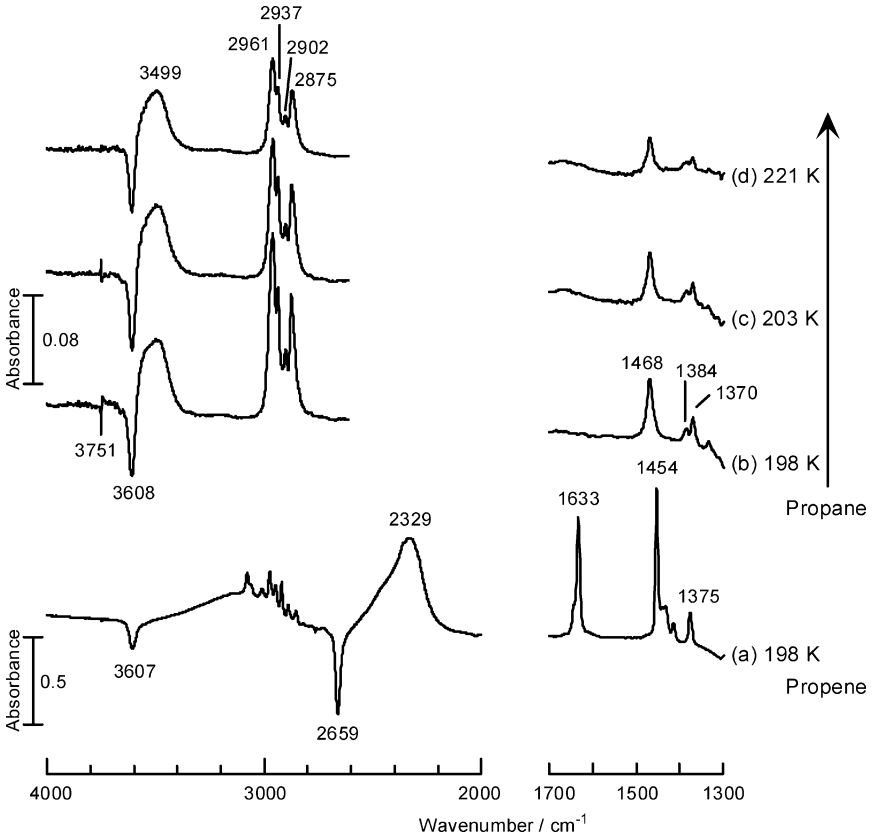

Figure 5. IR spectra of (a) propene and (b−d) propane on ferrierite introduced at 170 K followed by gradual warming under evacuation: (a) 198, (b) 198, (c) 203, and (d) 221 K.

conversion of isolated OH to OH groups hydrogen bonded with the alkyl groups of ethane (alkyl−OH adsorption), which appears as a complementary peak at 3499 cm^{-1}.[4,25,28] Peaks attributable to ν(CH) of ethane are observed at 2850−3000 cm^{-1}, and the δ(CH) peaks are present at 1370 and 1465 cm^{-1}. The dip at 3611 cm^{-1} and peak at 3499 cm^{-1} observed at 180 K indicate that the micropores are accessible to ethane at this temperature. Desorption of ethane was observed as the temperature was increased to 218 K under evacuation, as recognized by a weakening of the ν(CH) and δ(CH) peaks of adsorbed ethane, a shallowing of the dip due to acidic OH (3611 cm^{-1}), and weakening of the peak due to acidic OH groups hydrogen bonded with ethane (3499 cm^{-1}).

In the case of propane (Figure 5b−d), the appearance of a dip at 3608 cm^{-1} due to isolated acidic OH groups at 198 K indicates that the propane entered the micropores at this temperature. Similarly, a dip appeared at 3751 cm^{-1}, indicating adsorption to surface silanol groups. Increasing the temperature to 203 K (Figure 5c) eliminated propane adsorption on silanol groups, while the amount of adsorption on acidic OH groups remained almost unchanged. A further increase in temperature to 221 K resulted in the desorption of propane from the acidic OH groups, as indicated by a weakening of the 3608 cm^{-1} dip and 3500 cm^{-1} peak.

In contrast, as shown in Figure 5a, only adsorption on acidic OH groups was observed for propene, with no adsorption on silanol even at 198 K.[25] Therefore, propene appears to enter the micropores of ferrierite in the absence of considerable energy barriers, whereas propane must overcome much larger energy barriers to enter the micropores despite having the same carbon number.

Behavior similar to that of propane was observed for *n*-butane (Figure 6). The dips at 3751 and 3613 cm^{-1} due to adsorption

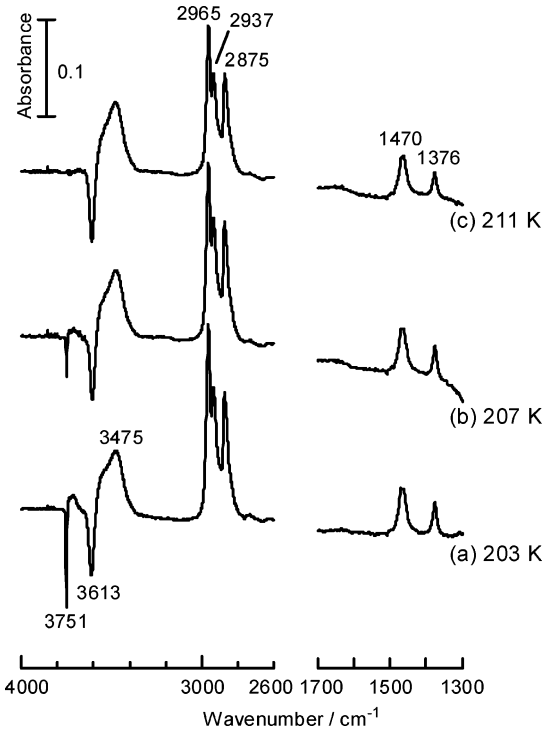

Figure 6. IR spectra of *n*-butane on ferrierite introduced at 170 K followed by gradual warming under evacuation: (a) 203, (b) 207, and (c) 211 K.

on silanol groups and acidic OH groups were both observed at 203 K. As the temperature was increased to 207 K, the adsorption of *n*-butane on silanol groups decreased to about half that at 203 K, and then disappeared at 211 K, whereas the amount of adsorption on acidic OH groups remained almost

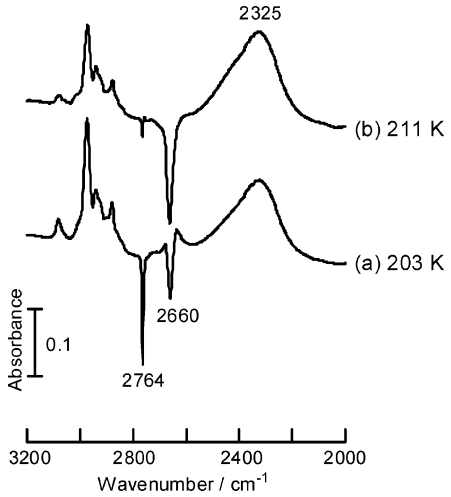

Figure 7. IR spectra of 1-butene on ferrierite introduced at 170 K followed by gradual warming under evacuation: (a) 203 and (b) 211 K.

unchanged. The disappearance of the dip at 3751 cm^{-1} at 211 K indicates that the *n*-butane molecules adsorbed on silanol groups on the external surface intruded into the micropores or were evacuated after desorption.

In the case of 1-butene on deuterated ferrierite, the dip due to OD of deuterated silanol at 2764 cm^{-1} was present at 203 K but disappeared at 211 K (Figure 7).[25] At this elevated temperature, the dip at 2660 cm^{-1} due to acidic OD groups strengthened as the density of adsorbed 1-butene on acidic OD groups increased, while the total adsorption of 1-butene (indicated by the bands at 2850−3100 cm^{-1}) decreased. As 1-butene adsorption was performed under continuous evacuation, additional adsorption from the gas phase was not considered. Therefore, the increase in the amount of adsorbed 1-butene on acidic OH groups is attributable to the conversion of 1-butene molecules adsorbed on the external surface. In the case of *n*-butane, however, although the dip due to isolated acidic OH groups and the peak due to hydrogen-bonded acidic OH groups remained relatively unchanged, the total amount of adsorbed *n*-butane decreased, as indicated by the weakening of the ν-(CH) (2800−3000 cm^{-1}) and δ(CH) (1300−1500 cm^{-1}) bands of *n*-butane. That is, the majority of *n*-butane molecules adsorbed on the external surface are considered to desorb by evacuation with increasing temperature.

Silanol adsorption was observed for propane and *n*-butane below 200 K, but not for ethane. At 203 K, about 20% of acidic OH groups in micropores are estimated to have been bonded to propane or *n*-butane. Although the remaining (80%) acidic OH groups were still capable of adsorbing propane or *n*-butane, less stable adsorption on silanol was observed. This suggests the presence of energy barriers against the intrusion of propane and *n*-butane into the micropores, similar to the case of *n*-butene.[25] For *n*-butene, a large energy barrier for the diffusion of molecules into the micropores causes *n*-butene molecules to preferably adsorb onto the external surface.[26] Although such energy barriers are also expected for propane and *n*-butane, other barriers are also considered below.

3.1.2. Adsorption of n-Alkane in Ferrierite Micropores. If energy barriers are the only obstacle to the intrusion of molecules into the micropores from the external surface, adsorption on acidic OH groups in the micropores should follow first-order kinetics. However, the experimental adsorption histories for *n*-butene did not exhibit linearity, instead suggesting a diffusion-limited process for intrusion into micropores.

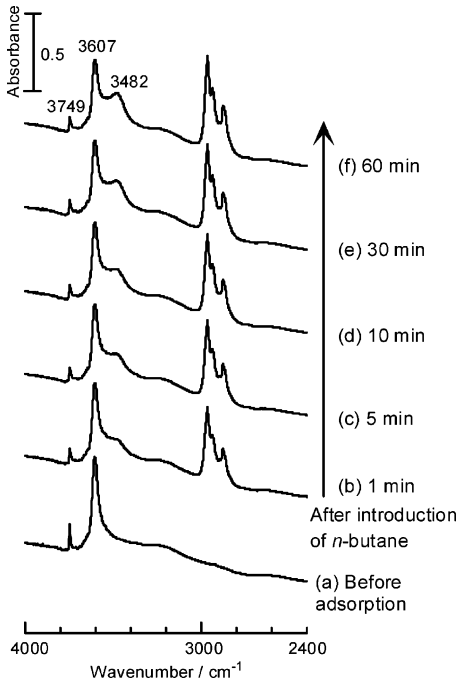

Figure 8. IR spectra of *n*-butane on ferrierite at 253 K (a) before adsorption and (b) 1, (c) 5, (d) 10, (e) 30, and (f) 60 min after introduction.

Consequently, the energy barriers against the intrusion of *n*-butene into the micropores appear to correspond to a diffusion step inside the micropores.[26] However, the results above suggested the presence of observable energy barriers for propane and *n*-butane with regard to adsorption to acidic OH groups inside the micropores. Considering the results for *n*-butene, the energy barriers for both propane and *n*-butane are expected to be related to diffusion into the micropores, although convincing evidence has yet to be obtained. To examine the effect of diffusion in the step with the apparent energy barrier in more detail, adsorption histories were measured for propane and *n*-butane similarly to the case for *n*-butene.

The adsorption histories for ferrierite micropores shown here were measured without evacuation in the presence of gaseous alkane molecules at a constant temperature of 233, 243, 253, or 263 K. Background spectra were measured, and then 20 μmol of propane or *n*-butane was introduced and the adsorption in micropores measured in an atmosphere of gas-phase alkane (1.2 Torr). As the acidic OH groups in ferrierite have been confirmed to exist only within the micropores,[7] the amount of alkane entering the micropores can be estimated from the rate of decrease in the density of isolated acidic OH groups or the fractional coverage of isolated acidic OH groups.

The sequential IR spectra of *n*-butane on ferrierite at 253 K are shown in Figure 8, without background subtraction. Comparing the spectra measured before and after adsorption, the peak at 3749 cm^{-1} due to silanol groups on the external surface immediately weakened by about half, but then remained relatively constant thereafter. On the other hand, the band at 3607 cm^{-1} attributable to acidic OH groups decreases gradually over time, accompanied by a gradual strengthening of the band at 3482 cm^{-1} due to acidic OH groups hydrogen bonded with *n*-butane, indicating gradual intrusion of *n*-butane into the micropores.

The fractional coverage of acidic OH groups for the adsorption of propane and *n*-butane was measured at between 233 and 263 K, and the histories are plotted in Figure 9. Pressure dependence of *n*-butane was not observed for the adsorption

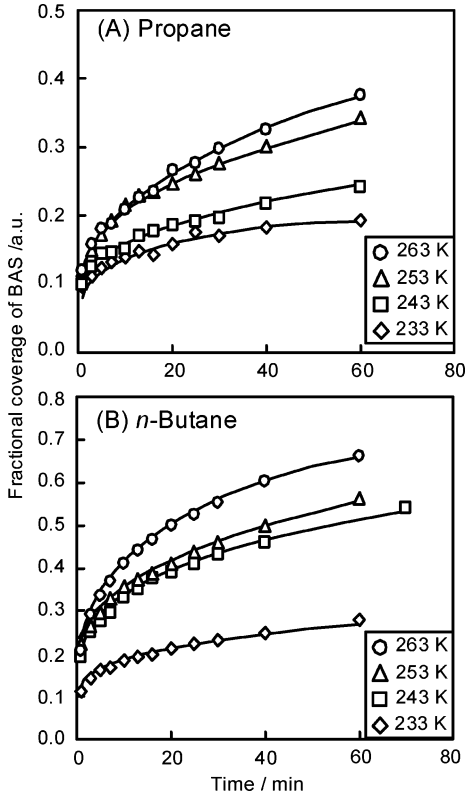

Figure 9. Fractional coverage of acidic OH groups on ferrierite after introduction of (A) propane and (B) *n*-butane.

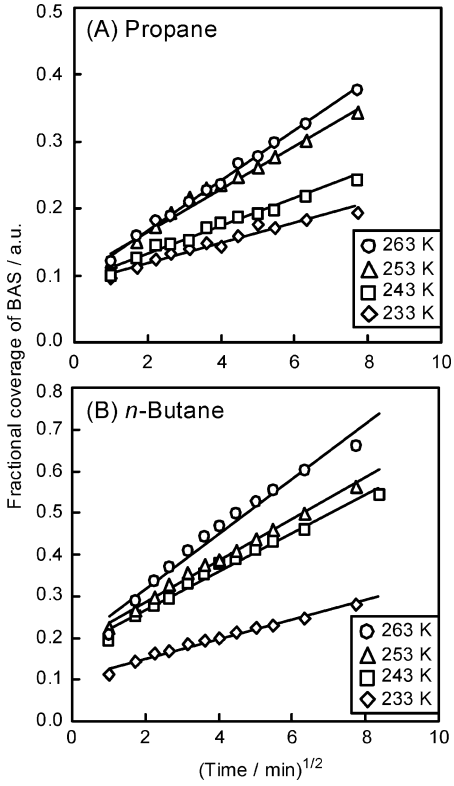

Figure 10. Fractional coverage of (A) propane and (B) *n*-butane adsorbed on acidic OH groups of ferrierite plotted against square root of time.

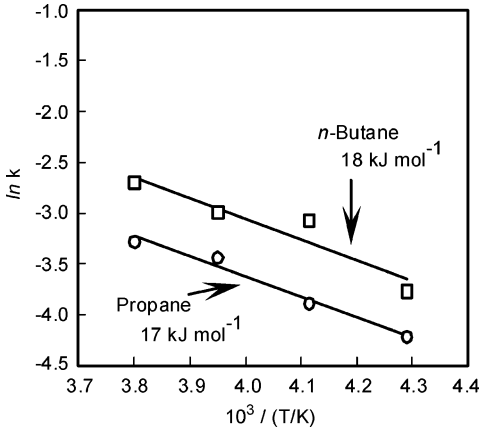

Figure 11. Arrhenius plots by rate constant of diffusion of propane and *n*-butane obtained from Figure 10.

on BASs. These results show the same features as for *n*-butene;[26] that is, the adsorption histories for acidic OH groups correspond not to a first-order process but to a diffusion process. Therefore, the rate-determining step of adsorption of propane and *n*-butane in the micropores of ferrierite is considered to be not the step for intrusion into the micropores from external surface, but the step for diffusion inside the micropores. For diffusion as the rate-determining step, under the present experimental conditions of zero initial concentration in the micropores and constant concentration externally, the adsorption M_t of alkanes on acidic OH groups over time is given by[32]

$$M_t = kt^{1/2} \quad (1)$$

where k is the rate constant of diffusion. Dividing both sides of eq 1 by the amount of acidic OH groups N, the left side of the equation gives the fractional coverage of acidic OH groups, which is plotted against the square root of time in Figure 10. The variation in fractional coverage is linear with respect to the square root of time, confirming that the energy barrier against intrusion into the micropores is the diffusion step inside the micropores. The slopes of the plots in Figure 10 corresponding to the rate constant of diffusion were estimated at each temperature. The activation energies for the diffusion of propane and *n*-butane in ferrierite micropores were then estimated from the Arrhenius plots shown in Figure 11, giving values of 17 and 18 kJ mol^{-1} for propane and *n*-butane, respectively. These values are summarized in Table 2 together with previous results for *n*-butene. The error of these results was ±2 kJ mol^{-1} for both alkanes.

Extrapolating the fractional coverage histories back to the initial time, the fractional coverage of acidic OH groups should be zero. However, Figure 10 does not give this result. In the adsorption of branched alkanes in ferrierite micropores,[33] 2-methylalkane was unable to enter the micropores and blocked the entrances to the micropores. However, 2-methylalkane could interact with a small fraction of the acidic OH groups of ferrierite via a constituent alkyl group, causing the acidic OH groups near the entrance of the pores to be consumed immediately after the introduction of 2-methylalkane. This suggests a weaker energy

TABLE 2: Activation Energies for Diffusion of *n*-Alkanes and *n*-Alkenes on Ferrierite

adsorbate	E_a/kJ mol^{-1}
propane	17
n-butane	18
propylene	*a*,*b*
1-butene	22[a]
cis-2-butene	28[a]
trans-2-butene	*a*,*b*

[a] Values obtained by IR measurement.[23] [b] The activation energy for diffusion could not be measured in the present study because of smaller activation energy.

TABLE 3: Heats of Adsorption for Alkanes and Alkenes on the Acidic OH Groups of Ferrierite and ZSM-5, and Silanol Groups of SiO_2

	acidic OH groups				silanol SiO_2
	ferrierite		ZSM-5		
	IR	calorimetric[a]	IR	calorimetric[b]	IR
ethane	37		38		17
propane	52	49	45	46	23
n-butane	63	59	53	58	27
isobutane	c		48	52	23
ethene	d		d		19
propylene	d		d		26
1-butene	d		d		30
cis-2-butene	d		d		32
trans-2-butene	d		d		36

[a] Values obtained from ref 29. [b] Values obtained from ref 30. [c] Heats of adsorption for isobutane on acidic OH groups could not be measured because it did not intrude into the micropores of ferrierite below room temperature. [d] Heats of adsorption for alkenes could not be measured because of their reaction on acidic OH groups.

barrier against the adsorption of 2-methylalkane on acidic OH groups near the entrance of the micropores. Thus, propane and *n*-butane may be able to interact with acidic OH groups near the entrance of the micropores with a weaker energy barrier, meaning that the consumption of isolated acidic OH groups immediately after the introduction of *n*-alkane may be unrelated to diffusion. In this case, only part of the molecules may enter fully into the micropores, with part of the molecule unable to enter the micropore.[33]

3.1.3. Heat of Alkane and Alkene Adsorption on Ferrierite, ZSM-5, and SiO_2. The activation energies for the diffusion of propane and *n*-butane into the micropores of ferrierite were obtained to compare with those for 1-butene and *cis*-2-butene (22 and 28 kJ mol^{-1}, respectively).[26] Since the activation energies for diffusion may depend on the heat of adsorption, the heat of alkane and alkene adsorption on silanol and BASs in zeolites is considered to be useful for investigating the detailed diffusion processes in the micropores. The heat of adsorption was obtained for ferrierite, ZSM-5, and amorphous silica. As the heat of alkene adsorption cannot be measured for ferrierite and ZSM-5 due to acid-catalyzed reactions, measurements were made only for the adsorption of C_2-C_4 alkanes on the acidic OH groups of ferrierite and ZSM-5.

The heat of C_2-C_4 alkane and alkene adsorption was measured for silica to estimate the heat of adsorption on silanol groups on the external surface of zeolites. The fractional coverage was estimated from the ν(OH) peak of acidic OH groups and silanol groups. The experimental conditions are summarized in Table 1. The heat of adsorption on each catalyst was estimated by the Clausius−Clapeyron equation obtained from the adsorption isotherms. The results are summarized in Table 3, together with those obtained from calorimetric measurements.[29,30] The accuracy of the IR measurement of the heat of adsorption was ± 1 kJ mol^{-1}. The IR results are very similar to the calorimetric results, with the difference most probably due to the different Si/Al ratios used for the zeolites (Si/Al = 50 in the present study and 35 in the literature[30]). Therefore, the IR results are considered to be reliable. The heat of adsorption for isobutane on the acidic OH groups of ferrierite could not be measured because isobutane is unable to enter the micropores of ferrierite, as reported previously.[6,7,33]

3.1.4. Diffusion of Alkane and Alkene in Ferrierite Micropores. From the study of *n*-butene, there are two possible interpretations for the energy barriers of diffusion as described in the Introduction: (i) the energy for desorption from BASs (Figure 3b) or (ii) the energy for migration on the wall (Figure 3a). As the heat of adsorption could not be measured for alkene on BASs, the activation energies for the diffusion of *n*-butene could not be compared with the heat of adsorption for *n*-butene. As such, the rate-determining step for diffusion could not be clarified from the results for *n*-butene adsorption.

Comparison of the results for alkanes and *n*-butene would be valuable, because although the carbon numbers of propane/propene and *n*-butane/*n*-butene are the same, a significant difference in the activation energies for diffusion has been indicated by this and previous studies.[25,26] The activation energies for diffusion increase in the order of propene and *trans*-2-butene ≪ propane, *n*-butane, 1-butene, and *cis*-2-butene.

The diffusion of propene and *trans*-2-butene in the micropores of ferrierite occurs much more rapidly than for the other *n*-butenes, and therefore could not be measured under the present experimental conditions. However, the activation energies for the diffusion of propane and *n*-butane were sufficiently large to be observed under the same experimental conditions. It has been reported based on molecular modeling of DD3R zeolite that the activation energy for the diffusion of propane is larger than that of propene.[24] If the activation energy for diffusion depends on the heat of adsorption, then the heat of adsorption for propane and *n*-butane should be larger than that for *trans*-2-butene. Although the heat of adsorption on acidic OH groups could not be compared for propane and *trans*-2-butene because the heat of adsorption of the latter could not be estimated, the heat of adsorption of those molecules on silanol groups is considered to increase in the same order as on acidic OH groups. From Table 3, *trans*-2-butene has a larger heat of adsorption on silanol groups than either propane or *n*-butane, suggesting that the activation energy for diffusion in micropores is not dependent on the heat of adsorption on BASs, instead being related more closely to the molecular shape of alkane and alkene. Thus, the rate-determining step for diffusion is concluded to be (a) in Figure 3, based on a comparison of the results for *n*-butene and alkane. This could not have been achieved using the results of *n*-butene alone.

3.2. Elementary Adsorption. A diffusion-limited adsorption process was observed by IR measurements for propane, *n*-butane, 1-butene, and *cis*-2-butene on ferrierite. Although the diffusion process could not be experimentally observed for 1-butene on ZSM-5, two adsorption structures (wall adsorption and alkyl−OH adsorption) were observed in the micropores at temperatures lower than that of π-adsorption.[4] As the difference in the observed behavior over ferrierite and ZSM-5 is considered to be due to the difference in the pore diameter of the zeolites, the adsorption of 1-butene on mordenite, which has even larger micropores, was examined to further the investigation.

3.2.1. Adsorption of 1-Butene on Mordenite. After the adsorption of 20 μmol of 1-butene on deuterated mordenite at 170 K, IR spectra were measured while the sample was warmed gradually under evacuation. The IR results are shown as background-subtracted spectra in Figure 12. Background spectra were obtained as the pretreated mordenite was cooled to 170 K prior to the introduction of 1-butene. A large dip at 2668 cm^{-1} due to the decrease in isolated acidic OD groups was observed at 185 K, complemented by the emergence of a peak due to acidic OD groups hydrogen bonded with 1-butene around 2000−2500 cm^{-1}. Therefore, 1-butene π-adsorbs to BASs in the micropores of mordenite at 185 K. However, interaction between the OD groups and the alkyl groups of 1-butene, as indicated by the band at 2500−2600 cm^{-1}, was not observed. Moreover, only the 1628 cm^{-1} peak due to ν(C═C) of 1-butene

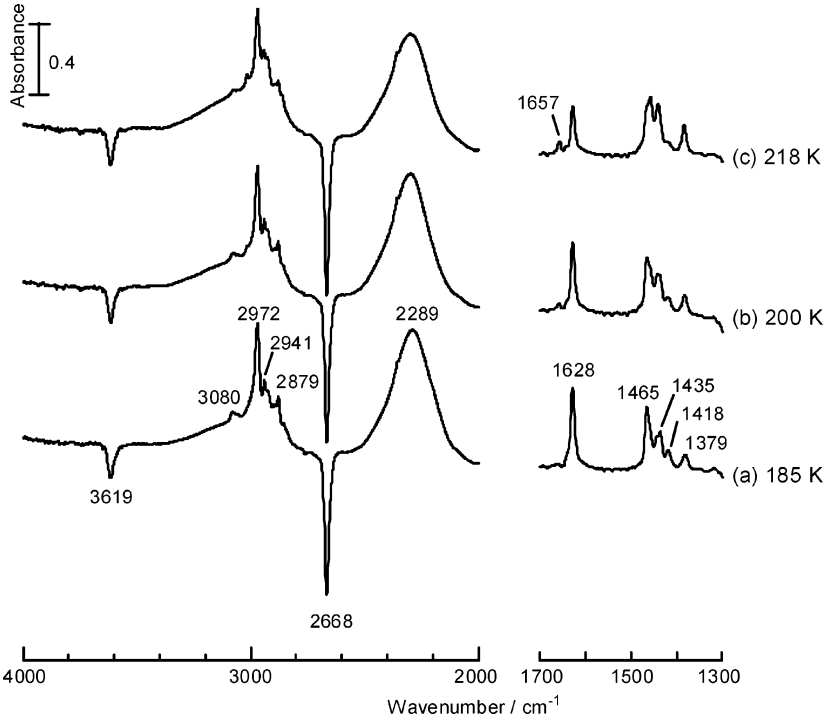

Figure 12. IR spectra of 1-butene on mordenite introduced at 170 K followed by gradual warming under evacuation: (a) 185, (b) 200, and (c) 218 K.

representing π-adsorption was observed; wall interaction indicated by a peak at 1642 cm^{-1} did not occur.[3] Although a band at 1657 cm^{-1} is observed at 218 K, this peak is attributed to ν(C═C) of *trans*-2-butene isomerized from 1-butene.[2,3,34] This isomerization resulted in a change in the ν(CH) (2900−3100 cm^{-1}) and δ(CH) (1400−1500 cm^{-1}) bands at 218 K. Thus, alkyl adsorption and wall interaction, which were observed on ZSM-5, were not observed on mordenite at 185 K, in the same temperature region. Furthermore, no species were observed to adsorb onto silanol groups on the external surface, supporting the small energy barrier for the diffusion of molecules into the micropores.

3.2.2. Observation of Elementary Adsorption Process. The observed elementary adsorption process differed depending on the zeolites and molecules examined. While only the π-interacted species of 1-butene appeared on mordenite at 180 K, wall interaction and alkyl adsorption were observed on ZSM-5 at the same temperature. The diffusion process in the micropores was observed for ferrierite, revealing that the entrances of micropores become blocked by diffusing molecules, causing molecules that could not intrude into the micropores to be detected as species adsorbed on silanol groups on the external surface. The presence or absence of experimentally observable diffusion processes on ferrierite is controlled by the size of the adsorbing molecule and the pore diameter of the ferrierite. The activation energy for diffusion was also found to vary depending on the adsorbing molecules, with the rate-determining step corresponding to Figure 3a for relatively large molecules (compared to the pore size) and Figure 3b for smaller molecules.

The experimental observation of wall adsorption and alkyl−OH adsorption is dependent on the accessibility of π-electrons of alkene to the acidic OH groups on the zeolites. Molecular models of 1-butene in the micropores of ferrierite, ZSM-5, and mordenite are shown in Figure 13. Although 1-butene molecules appear to come into close contact with all the walls of the micropores in ZSM-5, the contact is not as good in mordenite. It is considered that the acidic OH groups are restrained from approaching the π-electron of the C═C bond due to steric hindrance between the alkyl groups of *n*-butene and the walls of the micropores. Therefore, there is a larger energy barrier to π-adsorption in ZSM-5 than in mordenite, with the result that alkyl adsorption is more likely to be observed in ZSM-5.[4] While 1-butene also seems to be influenced by steric hindrance of the pore walls in ferrierite (Figure 13), alkyl adsorption was not observed because the molecules that overcome the energy barrier for diffusion into the micropores have sufficient energy to form π-adsorption bonds at the relevant temperatures.

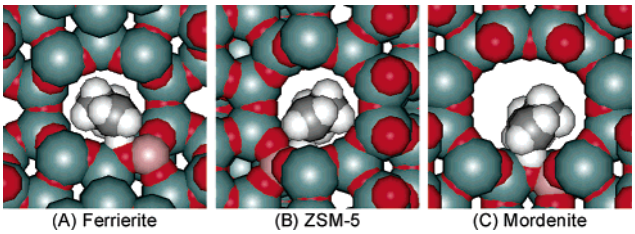

Figure 13. Influence of pore structure on adsorption of 1-butene on (A) ferrierite, (B) ZSM-5, and (C) mordenite.

As the rate-determining step for the formation of the most stable π-adsorption bond differs depending on the type of zeolite and adsorbing molecule, the elementary adsorption processes could be observed and clarified by comparing the adsorption of alkanes and alkenes on three types of zeolites.

4. Conclusion

The adsorption of alkanes and alkenes on three types of zeolite with different pore sizes were compared at low temperatures (below 300 K) based on FTIR spectroscopy. Propane and *n*-butane were observed to adsorb onto silanol groups on the external surface of ferrierite, indicating the existence of significant energy barriers preventing the alkanes from entering the micropores. This behavior is similar to that of *n*-butene, and is concluded to be related to the nature of alkane diffusion into the micropores. The activation energies for the diffusion

of propane and *n*-butane were estimated to be 17 and 18 kJ mol^{-1}, respectively. Comparison of the estimated diffusion activation energies for alkane with alkene revealed that the rate-determining step for diffusion depends not on the heat of adsorption for molecules adsorbing to BASs, but on molecular size and pore diameter. Diffusion was found to the rate-determining step due to the size-limited migration of molecules on the internal walls of micropores.

Various types of steric hindrance occur, controlled by the pore size, and a dependence of elementary adsorption processes on the pore size of the zeolites was observed. While only π-adsorbed species were observed for 1-butene adsorption on mordenite, which has large micropores, alkyl adsorption was observed for 1-butene adsorption on ZSM-5, which has slightly smaller pores. Species adsorbed on silanol groups on the external surface were present on ferrierite, with the smallest pores, as a transient state leading to diffusion into the micropores. In other words, the rate-determining step for the formation of the most stable π-adsorption structure was found to differ depending on the type of zeolite and molecule examined, and the elementary adsorption process could be interpreted based on this differing behavior.

References and Notes

(1) Weitkamp, J. *Solid State Ionics* **2000**, *131*, 175−188.
(2) Kondo, J. N.; Wakabayashi, F.; Domen, K. *J. Phys. Chem. B* **1997**, *101*, 5477−5479.
(3) Kondo, J. N.; Shao, L.; Wakabayashi, F.; Domen, K. *J. Phys. Chem. B* **1997**, *101*, 9314−9320.
(4) Kondo, J. N.; Wakabayashi, F.; Domen, K. *J. Phys. Chem. B* **1998**, *102*, 2259−2262.
(5) Ishikawa, H.; Yoda, E.; Kondo, J. N.; Wakabayashi, F.; Domen, K. *J. Phys. Chem. B* **1999**, *103*, 5681−5686.
(6) Kondo, J. N.; Ishikawa, H.; Yoda, E.; Wakabayashi, F.; Domen, K. *J. Phys. Chem. B* **1999**, *103*, 8538−8543.
(7) Kondo, J. N.; Yoda, E.; Ishikawa, H.; Wakabayashi, F.; Domen, K. *J. Catal.* **2000**, *191*, 275−281.
(8) Kondo, J. N.; Shao, L.; Wakabayashi, F.; Domen, K. *Catal. Lett.* **1997**, *47*, 129−133.
(9) Kondo, J. N.; Wakabayashi, F.; Domen, K. *Catal. Lett.* **1998**, *53*, 215−220.
(10) Van-Den-Begin, N.; Rees, L. V. C.; Caro, J.; Bulow, M. *Zeolites* **1989**, *9*, 287−292.
(11) Heink, W.; Karger, J.; Pfeifer, H.; Stallmach, F. *J. Am. Chem. Soc.* **1990**, *112*, 2175−2178.
(12) Hufton, J. R.; Ruthven, D. M. *Ind. Eng. Chem. Res.* **1993**, *32*, 2379−2386.
(13) Jobic, H.; Bee, M.; Kearley, G. J. *J. Phys. Chem.* **1994**, *98*, 4660−4665.
(14) Millot, B.; Methivier, A.; Jobic, H.; Moueddeb, H.; Bee, M. *J. Phys. Chem. B* **1999**, *103*, 1096−1101.
(15) Jobic, H. *J. Mol. Catal. A: Chem.* **2000**, *158*, 135−142.
(16) Anderson, B. G.; de Gauw, F. J. M. M.; Noordhoek, N. J.; van Ijzendoorn, L. J.; van Santen, R. A.; de Voigt, M. J. A. *Ind. Eng. Chem. Res.* **1998**, *37*, 815−824.
(17) Magusin, P. C. M. M.; Schuring, D.; van Oers, E. M.; de Haan, J. W.; van Santen, R. A. *Magn. Reson. Chem.* **1999**, *37*, S108−S117.
(18) Meunier, F. C.; Domokos, L.; Seshan, K.; Lercher, J. A. *J. Catal.* **2002**, *211*, 366−378.
(19) Pieterse, J. A. Z.; Veefkind-Reyes, S.; Seshan, K.; Domokos, L.; Lercher, J. A. *J. Catal.* **1999**, *187*, 518−520.
(20) Maginn, E. J.; Bell, A. T.; Theodorou, D. N. *J. Phys. Chem.* **1996**, *100*, 7155−7173.
(21) Runnebaum, R. C.; Maginn, E. J. *J. Phys. Chem. B* **1997**, *101*, 6394−6408.
(22) Schuring, D.; Jansen, A. P. J.; van Santen, R. A. *J. Phys. Chem. B* **2000**, *104*, 941−948.
(23) Jousse, F.; Auerbach, S. M.; Vercauteren, D. P. *J. Phys. Chem. B* **2000**, *104*, 2360−2370.
(24) ter Horst, J. H.; Bromley, S. T.; van Rosmalen, G. M.; Jansen, J. C. *Microporous Mesoporous Mater.* **2002**, *53*, 45−57.
(25) Yoda, E.; Kondo, J. N.; Wakabayashi, F.; Domen, K. *Appl. Catal., A* **2000**, *194*−*195*, 275−283.
(26) Kondo, J. N.; Yoda, E.; Wakabayashi, F.; Domen, K. *Catal. Today* **2000**, *63*, 305−308.
(27) Spoto, G.; Bordiga, S.; Ricchiardi, G.; Scarano, D.; Zecchina, A.; Borello, E. *J. Chem. Soc., Faraday Trans.* **1994**, *90*, 2827−2835.
(28) Makarova, M. A.; Ojo, A. F.; Karim, K.; Hunger, M.; Dwyer, J. *J. Phys. Chem.* **1994**, *98*, 3619−3623.
(29) Eder, F.; Lercher, J. A. *J. Phys. Chem. B* **1997**, *101*, 1273−1278.
(30) Eder, F.; Stockenhuber, M.; Lercher, J. A. *J. Phys. Chem. B* **1997**, *101*, 5414−5419.
(31) Lee, B. J.; Kondo, J. N.; Wakabayashi, F.; Domen, K. *Bull. Chem. Soc. Jpn.* **1998**, *71*, 2149−2152.
(32) Crank, J. In *The mathematics of diffusion*; Clarendon Press: Oxford, 1975; p 30.
(33) Yoda, E.; Kondo, J. N.; Wakabayashi, F.; Domen, K. *Phys. Chem. Chem. Phys.* **2003**, *5*, 3306−3310.
(34) Barnes, A. J.; Howells, J. D. R. *J. Chem. Soc., Faraday Trans. 2* **1973**, *69*, 532−539.